Optical Engineering

SPIEDigitalLibrary.org/oe

Receiver-aperture averaging of annular beams propagating through turbulent atmosphere

Canan Kamacıoğlu
Yahya Baykal
Erdem Yazgan

SPIE

Downloaded From: http://opticalengineering.spiedigitallibrary.org/ on 03/02/2017 Terms of Use: http://spiedigitallibrary.org/ss/termsofuse.aspx

Receiver-aperture averaging of annular beams propagating through turbulent atmosphere

Canan Kamacıoğlu
Çankaya University
Department of Mechatronics Engineering
Eskisehir Yolu, 29. km
06810, Yenimahalle, Ankara, Turkey
E-mail: cyazicioglu@cankaya.edu.tr

Yahya Baykal
Çankaya University
Department of Electronic and Communication Engineering
Eskisehir Yolu, 29. km
06810, Yenimahalle, Ankara, Turkey

Erdem Yazgan
Hacettepe University
Department of Electrical and Electronics Engineering
Beytepe Campus
06800, Ankara, Turkey

Abstract. For an annular beam incidence, the power scintillation index in a weakly turbulent atmosphere is derived at the receiver plane, which has a Gaussian aperture. Employing this derivation, the receiver-aperture averaging factor is evaluated. Annular beams are found more advantageous than the Gaussian beams when compared on receiver-aperture averaging basis. The analyses indicate that the effect of the aperture averaging increases as the propagation length increases. Increase in the structure constant and the secondary beam source size is observed to strengthen the effect of the aperture averaging when the primary beam source size is fixed. © *2013 Society of Photo-Optical Instrumentation Engineers (SPIE)* [DOI: 10.1117/1.OE.52.12.126103]

Subject terms: atmospheric propagation; atmospheric turbulence, scintillation.

Paper 130928 received Jun. 21, 2013; revised manuscript received Nov. 15, 2013; accepted for publication Nov. 18, 2013; published online Dec. 16, 2013.

1 Introduction

Free-space optical communication systems have gained a lot of interest for their high-data rate capacity, unregulated spectrum, low cost, and easy installation. However, optical beams are affected by the refractive index fluctuations known as the scintillations of the atmosphere. Laser-beam scintillations caused by atmospheric turbulence give rise to signal degradations in the optical communication link. For this reason, optical scintillation is one of the most important factors that determines the performance in an atmospheric optical communication link.

In the last years, there have been many studies in the literature to reduce the effect of scintillations that create an impairment effect on the optical communication link. Among these studies, the aperture averaging method, in which the beam is picked by a large collection aperture, has been an intriguing research area. The receiver-aperture averaging effects for the plane-wave intensity fluctuations have been studied by Tatarskii.[1] Wang et al. obtained a closed-form representation of the receiver-aperture averaging effect for a beam wave in turbulent atmosphere, where a Gaussian weighting function for the receiver aperture is utilized.[2] Ricklin and Davidson examined the effects of atmospheric turbulence strength and the degree of the source spatial coherence on the aperture averaging and the average bit error rate when the laser source is a Gaussian Schell beam.[3] Berman et al. analyzed the influence of beam fragmentation and wandering on the scintillation index for coherent and partially coherent beams and described the methods for significantly reducing the scintillation index.[4] Using the statistics of the exponentiated Weibull distribution family, the aperture averaging effect for the Gaussian beams in weak and moderate turbulence conditions is analyzed by Barrios and Dios.[5] Yi et al. investigated the average bit error rate of the on-off keying signals transmitted through turbulent atmosphere that is modeled by the exponentiated Weibull distribution.[6] The analytic expressions for the average intensity and the center of gravity of partially coherent annular beams with a decentered field propagating through atmospheric turbulence along a slant path are derived by Dou et al.[7] Using the extended Huygens–Fresnel principle, we formulated the power scintillation index of flat-topped beams propagating in a weak turbulent atmosphere and found the receiver-aperture averaging effect under flat-topped incidence.[8] In that study, we reported that in the same turbulent atmosphere, when the same large-sized receiver aperture is used, the reduction in the power scintillation index of the flatter beams is more than the reduction in the power scintillation index of the Gaussian beams, i.e., the receiver-aperture averaging effect is stronger when flat-topped beams are employed instead of Gaussian beams. When the flatness parameter is large, irrespective of the receiver-aperture size, strong receiver-aperture averaging is experienced. The effects of the annular beams on the reduction of the scintillations captured by a point detector are scrutinized at various turbulence strengths.[9–16]

In this article, by using the Huygens–Fresnel integral, we derive and evaluate the power scintillation index of the annular beams at the receiver having a Gaussian-shaped aperture and examine whether the use of incidences possessing annular-field profiles propagating in weakly turbulent atmosphere will be advantageous in the aperture averaging.

2 Formulation

The source field of an annular beam centered at the transverse source point $s_x = s_y = 0$ is

0091-3286/2013/$25.00 © 2013 SPIE

Downloaded From: http://opticalengineering.spiedigitallibrary.org/ on 03/02/2017 Terms of Use: http://spiedigitallibrary.org/ss/termsofuse.aspx

$$u(\mathbf{s}) = \sum_{\ell=1}^{2} A_\ell \exp\left(-\frac{s_x^2 + s_y^2}{2\alpha_{s\ell}^2}\right), \tag{1}$$

where s_x and s_y are the x and y components of the source plane vector $\mathbf{s} = (s_x, s_y)$, A_ℓ is the amplitude factor with $A_1 = -A_2 = 1$, $\alpha_{s\ell}$ is the Gaussian source size, and α_{s1} and α_{s2} denote the sizes of the outer (primary) and the inner (secondary) Gaussian beams, respectively. The average received intensity can be found by using the extended Huygens–Fresnel integral as[1]

$$\langle I(\mathbf{p})\rangle = \frac{1}{(\lambda L)^2}\int_{-\infty}^{\infty}\int_{-\infty}^{\infty}\int_{-\infty}^{\infty}\int_{-\infty}^{\infty} \mathbf{ds}_1^2 \mathbf{ds}_2^2 u(\mathbf{s_1}) u^*(\mathbf{s_2}) \times \exp\left\{\frac{jk}{2L}[(\mathbf{p}-\mathbf{s_1})^2 - (\mathbf{p}-\mathbf{s_2})^2] - \rho_0^{-2}(\mathbf{s}_1 - \mathbf{s}_2)^2\right\}, \tag{2}$$

where $k = 2\pi/\lambda$ is the wave number, λ is the wavelength, $j = (-1)^{1/2}$, $\rho_0 = (0.545 C_n^2 k^2 L)^{-3/5}$ is the coherence length of a spherical wave propagating in the turbulent medium, C_n^2 is the structure constant, L is the propagation length, "*" denotes the complex conjugate, and $\mathbf{p} = (p_x, p_y)$ is the receiver transverse coordinate. Performing the integrations in Eq. (2) by the repeated use of Eq. 3.323.2 of Ref. 17, we obtain

$$\langle I(\mathbf{p})\rangle = I_1 + I_2 + I_3 + I_4, \tag{3}$$

where

$$I_1 = I_{1x} I_{1y},$$

$$I_2 = I_{2x} I_{2y},$$

$$I_3 = I_{3x} I_{3y}, \quad \text{and}$$

$$I_4 = -I_{4x} I_{4y},$$

$$I_{1x} = C_1 v_1^{-1} y_1^{-1} \exp(-C_{2x} v_1^{-2}) \exp(-C_{2x} y_1^{-2} - C_{2x}\rho_0^{-4} v_1^{-4} y_1^{-2} + 2C_{2x}\rho_0^{-2} v_1^{-2} y_1^{-2}),$$

$$I_{2x} = C_1 v_1^{-1} y_2^{-1} \exp(-C_{2x} v_1^{-2}) \exp(-C_{2x} y_2^{-2} - C_{2x}\rho_0^{-4} v_1^{-4} y_2^{-2} + 2C_{2x}\rho_0^{-2} v_1^{-2} y_2^{-2}),$$

$$I_{3x} = C_1 v_2^{-1} y_3^{-1} \exp(-C_{2x} v_2^{-2}) \exp(-C_{2x} y_3^{-2} - C_{2x}\rho_0^{-4} v_2^{-4} y_3^{-2} + 2C_{2x}\rho_0^{-2} v_2^{-2} y_3^{-2}),$$

$$I_{4x} = C_1 v_2^{-1} y_4^{-1} \exp(-C_{2x} v_2^{-2}) \exp(-C_{2x} y_4^{-2} - C_{2x}\rho_0^{-4} v_2^{-4} y_4^{-2} + 2C_{2x}\rho_0^{-2} v_2^{-2} y_4^{-2}),$$

$$C_1 = \pi(\lambda L)^{-2},$$

$$C_{2x} = C_1 \pi p_x^2,$$

$$v_1 = (0.5\alpha_{s1}^{-2} + \rho_0^{-2} - j0.5kL^{-1})^{0.5},$$

$$v_2 = (0.5\alpha_{s2}^{-2} + \rho_0^{-2} - j0.5kL^{-1})^{0.5},$$

$$y_1 = (v_1 - v_1^{-2}\rho_0^{-4})^{0.5},$$

$$y_2 = (v_2 - v_1^{-2}\rho_0^{-4})^{0.5},$$

$$y_3 = (v_1 - v_2^{-2}\rho_0^{-4})^{0.5}, \quad \text{and}$$

$$y_4 = (v_2 - v_2^{-2}\rho_0^{-4})^{0.5}.$$

I_{1y}, I_{2y}, I_{3y}, I_{4y}, and C_{2y} are obtained by changing all the x subscripts to y in I_{1x}, I_{2x}, I_{3x}, I_{4x}, and C_{2x}, respectively.

The average power detected by a finite-sized receiver having a Gaussian aperture function is

$$\langle P\rangle = \int_{-\infty}^{\infty}\int_{-\infty}^{\infty}\langle I(\mathbf{p})\rangle \exp\left(-\frac{|\mathbf{p}|^2}{R^2}\right)\mathrm{d}^2\mathbf{p}, \tag{4}$$

where R is the radius of the receiver aperture. Substituting Eq. (3) in Eq. (4) and performing the integrations, we obtain

$$\langle P\rangle = P_1 + P_2 + P_3 + P_4, \tag{5}$$

where

$$P_1 = \pi v_1^{-2} y_1^{-2}(C_1^{-1}R^{-2} + v_1^{-2} + y_1^{-2} + y_1^{-2} v_1^{-4}\rho_0^{-4} - 2y_1^{-2} v_1^{-2}\rho_0^{-2})^{-1},$$

$$P_2 = \pi v_1^{-2} y_2^{-2}(C_1^{-1}R^{-2} + v_1^{-2} + y_2^{-2} + y_2^{-2} v_1^{-4}\rho_0^{-4} - 2y_2^{-2} v_1^{-2}\rho_0^{-2})^{-1},$$

$$P_3 = \pi v_2^{-2} y_3^{-2}(C_1^{-1}R^{-2} + v_2^{-2} + y_3^{-2} + y_3^{-2} v_2^{-4}\rho_0^{-4} - 2y_3^{-2} v_2^{-2}\rho_0^{-2})^{-1},$$

and

$$P_4 = \pi v_2^{-2} y_4^{-2}(C_1^{-1}R^{-2} + v_2^{-2} + y_4^{-2} + y_4^{-2} v_2^{-4}\rho_0^{-4} - 2y_4^{-2} v_2^{-2}\rho_0^{-2})^{-1}.$$

The average of the square of the power as detected by a finite-sized receiver having a Gaussian aperture function is found as[2]

$$\langle P^2\rangle = \int_{-\infty}^{\infty}\int_{-\infty}^{\infty}\int_{-\infty}^{\infty}\int_{-\infty}^{\infty}\langle I(\mathbf{p_1}) I(\mathbf{p_2})\rangle \times \exp\left(-\frac{|\mathbf{p_1}|^2 + |\mathbf{p_2}|^2}{R^2}\right)\mathrm{d}^2\mathbf{p_1}\mathrm{d}^2\mathbf{p_2}, \tag{6}$$

where

Downloaded From: http://opticalengineering.spiedigitallibrary.org/ on 03/02/2017 Terms of Use: http://spiedigitallibrary.org/ss/termsofuse.aspx

$$\langle I(\mathbf{p_1})I(\mathbf{p_2})\rangle = \frac{1}{(\lambda L)^4}\int_{-\infty}^{\infty}\int_{-\infty}^{\infty}\mathrm{d}^2\mathbf{s}_1\int_{-\infty}^{\infty}\int_{-\infty}^{\infty}\mathrm{d}^2\mathbf{s}_2 \times\int_{-\infty}^{\infty}\int_{-\infty}^{\infty}\mathrm{d}^2\mathbf{s}_3\int_{-\infty}^{\infty}\int_{-\infty}^{\infty}\mathrm{d}^2\mathbf{s}_4 u(\mathbf{s}_1)u*(\mathbf{s_2})u(\mathbf{s}_3)u*(\mathbf{s_4}) \times\exp\left[\frac{jk}{2L}(|\mathbf{p_1}-\mathbf{s_1}|^2-|\mathbf{p_1}-\mathbf{s_2}|^2+|\mathbf{p_2}-\mathbf{s_3}|^2-|\mathbf{p_2}-\mathbf{s_4}|^2\right] \times\langle\exp[\psi(\mathbf{s}_1,\mathbf{p_1})+\psi^*(\mathbf{s}_2,\mathbf{p_1})+\psi(\mathbf{s}_3,\mathbf{p_2})+\psi^*(\mathbf{s}_4,\mathbf{p_2})\rangle, \tag{7}$$

where $\psi(\mathbf{s},\mathbf{p})$ is the Rytov solution of the random part of the complex phase of a spherical wave propagating from the source point $(\mathbf{s}, z=0)$ to the receiver point $(\mathbf{p}, z=L)$, with z being the propagation axis. The fourth-order medium coherence function given in the last line of Eq. (7) is expressed as[2]

$$\exp\left[-\frac{1}{2}D_\psi(\mathbf{s}_1-\mathbf{s}_2,0)-\frac{1}{2}D_\psi(\mathbf{s}_1-\mathbf{s}_4,\mathbf{p}_d)-\frac{1}{2}D_\psi(\mathbf{s}_2-\mathbf{s}_3,\mathbf{p}_d) -\frac{1}{2}D_\psi(\mathbf{s}_3-\mathbf{s}_4,0)+\frac{1}{2}D_\psi(\mathbf{s}_2-\mathbf{s}_4,\mathbf{p}_d)+\frac{1}{2}D_\psi(\mathbf{s}_1-\mathbf{s}_3,\mathbf{p}_d) +2B_\chi(\mathbf{s}_2-\mathbf{s}_4,\mathbf{p}_d)+2B_\chi(\mathbf{s}_1-\mathbf{s}_3,\mathbf{p}_d)+jD_{\chi S}(\mathbf{s}_2-\mathbf{s}_4,\mathbf{p}_d) -jD_{\chi S}(\mathbf{s}_1-\mathbf{s}_3,\mathbf{p}_d)\right], \tag{8}$$

where

$\mathbf{p}_d = \mathbf{p}_1 - \mathbf{p}_2$,

$D_\psi(\mathbf{s}_d,\mathbf{p}_d) = 2\rho_0^{-2}(\mathbf{s}_d^2+\mathbf{s}_d.\mathbf{p}_d+\mathbf{p}_d^2)$,

$B_\chi(\mathbf{s}_d,\mathbf{p}_d) = \sigma_{\chi_s}^2 - 0.5D_\chi(\mathbf{s}_d,\mathbf{p}_d)$,

$D_\chi(\mathbf{s}_d,\mathbf{p}_d) = (\rho_0^{-2}-\rho_\chi^{-2})\quad(\mathbf{s}_d^2+\mathbf{s}_d.\mathbf{p}_d+\mathbf{p}_d^2)$,

$D_{\chi S}(\mathbf{s}_d,\mathbf{p}_d) = \rho_{\chi S}^{-2}(\mathbf{s}_d^2+\mathbf{s}_d.\mathbf{p}_d+\mathbf{p}_d^2)$,

$\mathbf{s}_d = \mathbf{s}_r - \mathbf{s}_q$ with

$r = 1, 2, 3, 4$ and

$q = 2, 3, 4$,

$\sigma_{\chi_s}^2 = 0.124k^{7/6}C_n^2L^{11/6}$,

$\rho_{\chi S}^{-2} = 0.114C_n^2k^{13/6}L^{5/6}$, and

$\rho_\chi^{-2} = 0.425C_n^2k^{13/6}L^{5/6}$.

Employing Eqs. (1) and (8) in Eq. (7) and using the resulting Eq. (7) in Eq. (6), the formula for $\langle P^2\rangle$ is obtained. Applying Eq. 3.323.2 of Ref. 17 and performing the eightfold integration over the source transverse coordinates and the fourfold integration over the transverse receiver coordinates, we find

$$\langle P^2\rangle = \frac{\pi^6\exp(4\sigma_{xs}^2)}{(\lambda L)^4}\sum_{\ell=1}^{16}Q_\ell\frac{1}{\beta_\ell^2\gamma_\ell^2\varphi_\ell^2\delta_\ell^2\chi_\ell^2\vartheta_\ell^2}, \tag{9}$$

where

$$\beta_m^2 = \frac{1}{2\alpha_{s1}^2}-\frac{jk}{2L}+\frac{2}{\rho_0^2}-Y \quad \text{for } m=1,\ldots,8,$$

$$\beta_n^2 = \frac{1}{2\alpha_{s2}^2}-\frac{jk}{2L}+\frac{2}{\rho_0^2}-Y \quad \text{for } n=9,\ldots,16,$$

$Q_\ell = 1$ for all $\ell\times$ except $Q_3 = Q_{16} = -1$,

$$\theta_1^2 = \frac{1}{2\alpha_{s1}^2}+\frac{jk}{2L}+\frac{2}{\rho_0^2}-V,$$

$$\theta_2^2 = \theta_3^2 = \theta_4^2 = \theta_9^2 = \theta_{10}^2 = \theta_{11}^2 = \theta_{12}^2 = \theta_1^2,$$

$$\theta_5^2 = \frac{1}{2\alpha_{s2}^2}+\frac{jk}{2L}+\frac{2}{\rho_0^2}-V, \quad \theta_6^2 = \theta_7^2 = \theta_8^2 = \theta_{13}^2 = \theta_{14}^2 = \theta_{15}^2 = \theta_{16}^2 = \theta_5^2, \quad V = \frac{j}{\rho_{\chi S}^2}+\frac{1}{\rho_x^2}, \quad Y = -\frac{j}{\rho_{\chi S}^2}+\frac{1}{\rho_x^2},$$

$$\gamma_\ell^2 = -\frac{1}{\beta_\ell^2\rho_0^4}+\theta_\ell^2, \quad \varphi_\ell^2 = -\frac{1}{\gamma_\ell^2}\left(\frac{1}{\rho_0^2}-\frac{Y}{\beta_\ell^2\rho_0^2}\right)^2-\frac{Y^2}{\beta_\ell^2}+\varsigma_\ell^2,$$

$$\varsigma_1^2 = \frac{1}{2\alpha_{s1}^2}-\frac{jk}{2L}+\frac{2}{\rho_0^2}-Y,$$

$$\varsigma_2^2 = \varsigma_5^2 = \varsigma_6^2 = \varsigma_9^2 = \varsigma_{10}^2 = \varsigma_{13}^2 = \varsigma_{14}^2 = \varsigma_1^2, \quad \varsigma_3^2 = \frac{1}{2\alpha_{s2}^2}-\frac{jk}{2L}+\frac{2}{\rho_0^2}-Y, \quad \varsigma_4^2 = \varsigma_7^2 = \varsigma_8^2 = \varsigma_{11}^2 = \varsigma_{12}^2 = \varsigma_{15}^2 = \varsigma_{16}^2 = \varsigma_3^2,$$

$$\delta_\ell^2 = -\frac{1}{\varphi_\ell^2}\left[\frac{1}{\gamma_\ell^2}\left(-\frac{Y}{\beta_\ell^2\rho_0^2}+\frac{1}{\rho_0^2}\right)\left(\frac{1}{\beta_\ell^2\rho_0^4}-V\right)-\frac{Y}{\beta_\ell^2\rho_0^2}+\frac{1}{\rho_0^2}\right]^2 -\frac{1}{\gamma_\ell^2}\left(\frac{1}{\beta_\ell^2\rho_0^4}-V\right)^2-\frac{1}{\beta_\ell^2\rho_0^4}+\xi_\ell^2,$$

$$\xi_1^2 = \frac{1}{2\alpha_{s1}^2}+\frac{jk}{2L}+\frac{2}{\rho_0^2}-V, \quad \xi_3^2 = \xi_5^2 = \xi_7^2 = \xi_9^2 = \xi_{11}^2 = \xi_{13}^2 = \xi_{15}^2 = \xi_1^2,$$

$$\xi_2^2 = \frac{1}{2\alpha_{s2}^2}+\frac{jk}{2L}+\frac{2}{\rho_0^2}-V, \quad \xi_4^2 = \xi_6^2 = \xi_8^2 = \xi_{10}^2 = \xi_{12}^2 = \xi_{14}^2 = \xi_{16}^2 = \xi_2^2,$$

Downloaded From: http://opticalengineering.spiedigitallibrary.org/ on 03/02/2017 Terms of Use: http://spiedigitallibrary.org/ss/termsofuse.aspx

$$\chi_\ell^2 = \frac{1}{R^2} - \frac{B_\ell^2}{4\delta_\ell^2} - \frac{1}{4\varphi_\ell^2}\left\{\frac{1}{\gamma_\ell^2}\left[\frac{1}{\beta_\ell^2\rho_0^2}\left(Y-\frac{1}{\rho_0^2}\right)-\frac{1}{\rho_0^2}+V\right]\left(-\frac{Y}{\beta_\ell^2\rho_0^2}+\frac{1}{\rho_0^2}\right)-\frac{1}{\beta_\ell^2}\left(Y-\frac{1}{\rho_0^2}\right)Y+\frac{1}{\rho_0^2}-Y\right\}^2$$
$$+\frac{k^2}{4\varphi_\ell^2L^2}\left[\frac{1}{\gamma_\ell^2}\left(-\frac{Y}{\beta_\ell^2\rho_0^2}+\frac{1}{\rho_0^2}\right)\left(1-\frac{1}{\beta_\ell^2\rho_0^2}\right)+\frac{Y}{\beta_\ell^2}\right]^2-\frac{jk}{2\varphi_\ell^2L}\left\{\frac{1}{\gamma_\ell^2}\left[\frac{1}{\beta_\ell^2\rho_0^2}\left(Y-\frac{1}{\rho_0^2}\right)-\frac{1}{\rho_0^2}+V\right]\right.$$
$$\left.\times\left(-\frac{Y}{\beta_\ell^2\rho_0^2}+\frac{1}{\rho_0^2}\right)-\frac{1}{\beta_\ell^2}\left(-\frac{1}{\rho_0^2}+Y\right)Y+\frac{1}{\rho_0^2}-Y\right\}\left[\frac{1}{\gamma_\ell^2}\left(-\frac{Y}{\beta_1^2\rho_0^2}+\frac{1}{\rho_0^2}\right)\left(1-\frac{1}{\beta_1^2\rho_0^2}\right)+\frac{Y}{\beta_1^2}\right]$$
$$-\frac{1}{4\gamma_\ell^2}\left[\frac{1}{\rho_0^2\beta_\ell^2}\left(Y-\frac{1}{\rho_0^2}\right)-\frac{1}{\rho_0^2}+V\right]^2+\frac{k^2}{4\gamma_\ell^2L^2}\left(1-\frac{1}{\beta_\ell^2\rho_0^2}\right)^2-\frac{1}{2\gamma_\ell^2}\left[\frac{jk}{\beta_\ell^2\rho_0^2L}\left(Y-\frac{1}{\rho_0^2}\right)-\frac{1}{\rho_0^2}+V\right]$$
$$\times\left(1-\frac{1}{\beta_\ell^2}\frac{1}{\rho_0^2}\right)-\frac{1}{4\beta_\ell^2}\left(Y-\frac{1}{\rho_0^2}\right)^2+\frac{k^2}{4\beta_\ell^2L^2}+\frac{1}{2\beta_\ell^2}\left(Y-\frac{1}{\rho_0^2}\right)\frac{jk}{L}-\left(Y-\frac{2}{\rho_0^2}+V\right),$$

$$\vartheta_\ell^2 = \frac{k^2}{4\varphi_\ell^2L^2}-\frac{1}{4\varphi_\ell^2}\left\{\frac{1}{\gamma_\ell^2}\left[\frac{1}{\beta_\ell^2\rho_0^2}\left(Y-\frac{1}{\rho_0^2}\right)-\frac{1}{\rho_0^2}+V\right]\left(-\frac{Y}{\beta_\ell^2\rho_0^2}+\frac{1}{\rho_0^2}\right)-\frac{1}{\beta_\ell^2}\left(Y-\frac{1}{\rho_0^2}\right)Y+\frac{1}{\rho_0^2}-Y\right\}^2$$
$$-\frac{jk}{2\varphi_\ell^2L}\left\{\frac{1}{\gamma_\ell^2}\left[\frac{1}{\beta_\ell^2}\frac{1}{\rho_0^2}\left(-\frac{1}{\rho_0^2}+Y\right)-\frac{1}{\rho_0^2}+V\right]\left(-\frac{Y}{\beta_\ell^2\rho_0^2}+\frac{1}{\rho_0^2}\right)-\frac{1}{\beta_\ell^2}\left(Y-\frac{1}{\rho_0^2}\right)Y+\frac{1}{\rho_0^2}-Y\right\}$$
$$+\frac{1}{R^2}-\frac{F_\ell^2}{4\chi_\ell^2}-\frac{D_\ell^2}{4\delta_\ell^2}-\frac{1}{4\gamma_\ell^2}\left[\frac{1}{\rho_0^2\beta_\ell^2}\left(Y-\frac{1}{\rho_0^2}\right)-\frac{1}{\rho_0^2}+V\right]^2-\frac{1}{4\beta_\ell^2}\left(Y-\frac{1}{\rho_0^2}\right)^2-\left(Y-\frac{2}{\rho_0^2}+V\right),$$

$$B_\ell = E_\ell+\frac{jk}{\varphi_\ell^2L}\left[\frac{1}{\gamma_\ell^2}\left(\frac{1}{\rho_0^2}-\frac{Y}{\beta_\ell^2\rho_0^2}\right)\left(\frac{1}{\beta_\ell^2\rho_0^4}-V\right)-\frac{Y}{\beta_\ell^2\rho_0^2}+\frac{1}{\rho_0^2}\right]\left[\frac{1}{\gamma_\ell^2}\left(\frac{1}{\rho_0^2}-\frac{Y}{\beta_\ell^2\rho_0^2}\right)\left(1-\frac{1}{\beta_\ell^2\rho_0^2}\right)+\frac{Y}{\beta_\ell^2}\right]$$
$$+\frac{jk}{\gamma_\ell^2L}\left(\frac{1}{\beta_\ell^2\rho_0^4}-V\right)\left(1-\frac{1}{\beta_\ell^2\rho_0^2}\right)-\frac{jk}{\beta_\ell^2\rho_0^2L},$$

$$E_\ell = \frac{1}{\beta_\ell^2}\frac{1}{\rho_0^2}\left(-\frac{1}{\rho_0^2}+Y\right)+\frac{1}{\rho_0^2}-V+\frac{1}{\varphi_\ell^2}\left[\frac{1}{\gamma_\ell^2}\left(\frac{1}{\rho_0^2}-\frac{Y}{\beta_\ell^2\rho_0^2}\right)\left(\frac{1}{\beta_\ell^2\rho_0^4}-V\right)-\frac{Y}{\beta_\ell^2\rho_0^2}+\frac{1}{\rho_0^2}\right]$$
$$\times\left\{\frac{1}{\gamma_\ell^2}\left[\frac{1}{\beta_\ell^2\rho_0^2}\left(Y-\frac{1}{\rho_0^2}\right)-\frac{1}{\rho_0^2}+V\right]\left(\frac{1}{\rho_0^2}-\frac{Y}{\beta_\ell^2\rho_0^2}\right)-\frac{1}{\beta_\ell^2}\left(Y-\frac{1}{\rho_0^2}\right)Y+\frac{1}{\rho_0^2}-Y\right\}+\frac{1}{\gamma_\ell^2}\left(\frac{1}{\beta_\ell^2\rho_0^4}-V\right)\left[\frac{1}{\beta_\ell^2\rho_0^2}\left(Y-\frac{1}{\rho_0^2}\right)-\frac{1}{\rho_0^2}+V\right],$$

$$D_\ell = \frac{jk}{\varphi_\ell^2L}\left[\frac{1}{\gamma_\ell^2}\left(-\frac{1}{\beta_\ell^2}\frac{1}{\rho_0^2}Y+\frac{1}{\rho_0^2}\right)\left(\frac{1}{\beta_\ell^2\rho_0^4}-V\right)-\frac{1}{\beta_\ell^2}\frac{1}{\rho_0^2}Y+\frac{1}{\rho_0^2}\right]-E_\ell-\frac{jk}{L},$$

and

$$F_\ell = \frac{B_\ell D_\ell}{2\delta_\ell^2}-\frac{1}{2\varphi_\ell^2}\left\{\frac{1}{\gamma_\ell^2}\left[\frac{1}{\beta_\ell^2\rho_0^2}\left(Y-\frac{1}{\rho_0^2}\right)-\frac{1}{\rho_0^2}+V\right]\left(\frac{1}{\rho_0^2}-\frac{Y}{\beta_\ell^2\rho_0^2}\right)-\frac{1}{\beta_\ell^2}\left(Y-\frac{1}{\rho_0^2}\right)Y+\frac{1}{\rho_0^2}-Y\right\}^2$$
$$-\frac{1}{2\varphi_\ell^2}\left\{\frac{1}{\gamma_\ell^2}\left[\frac{1}{\beta_\ell^2\rho_0^2}\left(Y-\frac{1}{\rho_0^2}\right)-\frac{1}{\rho_0^2}+V\right]\left(\frac{1}{\rho_0^2}-\frac{Y}{\beta_\ell^2\rho_0^2}\right)-\frac{1}{\beta_\ell^2}\left(Y-\frac{1}{\rho_0^2}\right)Y+\frac{1}{\rho_0^2}-Y\right\}$$
$$\times\left[\frac{jk}{\gamma_\ell^2L}\left(\frac{1}{\rho_0^2}-\frac{Y}{\beta_\ell^2\rho_0^2}\right)\left(1-\frac{1}{\beta_\ell^2\rho_0^2}\right)+\frac{jk}{\beta_\ell^2L}Y\right]-\frac{jk}{2\varphi_\ell^2L}\left\{\frac{1}{\gamma_\ell^2}\left[\frac{1}{\beta_\ell^2\rho_0^2}\left(Y-\frac{1}{\rho_0^2}\right)-\frac{1}{\rho_0^2}+V\right]\times\left(\frac{1}{\rho_0^2}-\frac{Y}{\beta_\ell^2\rho_0^2}\right)\right.$$
$$\left.-\frac{1}{\beta_\ell^2}\left(-\frac{1}{\rho_0^2}+Y\right)Y+\frac{1}{\rho_0^2}-Y\right\}+\frac{k^2}{2\varphi_\ell^2L^2}\left[\frac{1}{\gamma_\ell^2}\left(\frac{1}{\rho_0^2}-\frac{Y}{\beta_\ell^2\rho_0^2}\right)\left(1-\frac{1}{\beta_\ell^2\rho_0^2}\right)+\frac{Y}{\beta_\ell^2}\right]-\frac{1}{2\gamma_\ell^2}\left[\frac{1}{\rho_0^2\beta_\ell^2}\left(Y-\frac{1}{\rho_0^2}\right)-\frac{1}{\rho_0^2}+V\right]^2$$
$$-\frac{jk}{2\gamma_\ell^2L}\left[\frac{1}{\beta_\ell^2\rho_0^2}\left(Y-\frac{1}{\rho_0^2}\right)-\frac{1}{\rho_0^2}+V\right]\left(1-\frac{1}{\beta_\ell^2\rho_0^2}\right)-\frac{1}{2\beta_\ell^2}\left(Y-\frac{1}{\rho_0^2}\right)^2+\frac{jk}{2\beta_\ell^2L}\left(Y-\frac{1}{\rho_0^2}\right)-2\left(Y-\frac{2}{\rho_0^2}+V\right).$$

Downloaded From: http://opticalengineering.spiedigitallibrary.org/ on 03/02/2017 Terms of Use: http://spiedigitallibrary.org/ss/termsofuse.aspx

The power scintillation is given by[18]

$$m_p^2 = \frac{\langle (P - \langle P \rangle)^2 \rangle}{\langle P \rangle^2} = \frac{\langle P^2 \rangle}{\langle P \rangle^2} - 1.$$

The receiver-aperture averaging factor G_R is defined as[18]

$$G_R = \frac{m_p^2}{m_p^2|_{R=0}}, \tag{11}$$

where $m_p^2|_{R=0}$ is the scintillation index for a point aperture.

3 Results

In this section, the effects of the radius of the receiver aperture, the propagation length, and the source size of the primary beam and the secondary beam on the power scintillation index and thus on the receiver-aperture averaging factor found analytically in the previous section are analyzed. To this end, the power scintillation index m_p^2 and the receiver-aperture averaging factor G_R are plotted according to the various values of the structure constant, the receiver-aperture radius, and the primary and the secondary beam source sizes by using Eqs. (10) and (11). In all the figures, $\lambda = 1.55$ μm is taken. Our results satisfy the scintillation index of annular beams[10,11] for the existing unapertured cases and the power scintillation index of a Gaussian beam propagating in turbulent atmosphere[2] as well. The receiver-aperture averaging factor versus the radius of the receiver aperture for different structure constant values is plotted in Fig. 1, in which $\alpha_{s1} = 5$ cm, $\alpha_{s2} = 2.5$ cm, and $L = 3$ km are taken. We observed from Fig. 1 that the effect of the receiver-aperture averaging increases with increasing values of the structure constant for all values of the receiver-aperture radius. In a turbulent medium for smaller propagation lengths, the annular beams do not carry energy on the propagation axis. As the propagation length increases, the intensity profile turns to a pure Gaussian shape.[19,20] In Fig. 1, the propagation length is taken as $L = 3$ km. Since the beam has an annular intensity profile, there is a first drop in Fig. 1. That means, from the first minimum point to the top, the beam size is much larger than the receiver aperture radius so that the received power is scaled by the receiver area. Then, the receiver becomes comparable

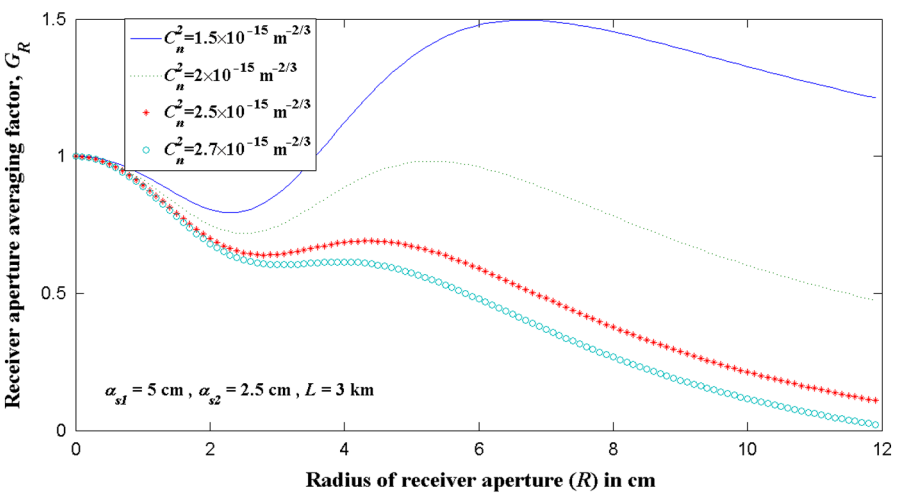

Fig. 1 The receiver-aperture averaging factor G_R versus the radius of the receiver aperture R at $\alpha_{s1} = 5$ cm, $\alpha_{s2} = 2.5$ cm, and $L = 3$ km for different C_n^2 values.

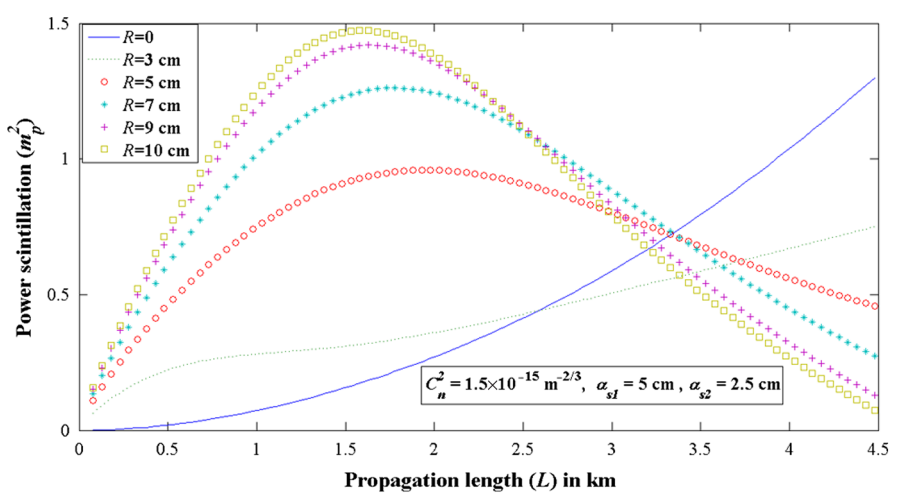

Fig. 2 Power scintillation versus the propagation length L at $C_n^2 = 1.5 \times 10^{-15}$ m$^{-2/3}$, $\alpha_{s1} = 5$ cm, and $\alpha_{s2} = 2.5$ cm for different R values.

Downloaded From: http://opticalengineering.spiedigitallibrary.org/ on 03/02/2017 Terms of Use: http://spiedigitallibrary.org/ss/termsofuse.aspx

to and larger than the beam size and captures more power. If Fig. 1 is examined against the effect of the radius of the receiver aperture, it is seen that the aperture averaging is more advantageous at relatively larger receiver-aperture sizes than at smaller apertures. The effect of the propagation length on the power scintillation of annular beams at different aperture sizes is investigated in Fig. 2, where the source size of the primary beam is $\alpha_{s1} = 5$ cm and the source size of the secondary beam is $\alpha_{s2} = 1.5$ cm. Figure 2 indicates that the power scintillation increases at smaller propagation lengths regardless of the radius of the receiver aperture, but at large propagation lengths, it starts to decrease for larger apertures. Examining at a fixed smaller propagation length, as the radius of the receiver aperture increases, the power scintillation also increases. However, this trend reverses at larger propagation lengths.[8] This means that the receiver-aperture averaging is not effective at smaller propagation lengths. In Fig. 3, the power scintillations of annular beams having different secondary beam source sizes are analyzed versus the propagation length, in which the source size of the primary beam is taken as $\alpha_{s1} = 5$ cm and the receiver aperture has a radius of $R = 6$ cm. It is observed that at a fixed propagation length, when the source size of the secondary beam increases, i.e., when the hollow core of the beam becomes wider, power scintillation increases. However, when propagation length increases considerably, the increasing secondary beam source size does not cause a significant difference on the power scintillations. The hollow core of the beam is filled, i.e., the annular optical field in turbulence eventually attains a pure Gaussian profile, as the propagation length increases.[19,20] For this reason, the increase in the secondary beam source sizes at large propagation lengths does not affect the power scintillation, since the beam field profile is no longer annular but rather Gaussian. Figure 4 shows the relation between the receiver-aperture averaging factor and the source size of the primary beam at different radii of the receiver aperture and different source sizes of the secondary beams at $L = 4$ km. Although the effect of the receiver-aperture averaging is not seen for very small source sizes of the primary beam, it becomes dominant when the source size of the primary beam increases to a certain value, i.e., $\alpha_{s1} = 4$ cm. Also, we conclude from Fig. 4 that the receiver-aperture averaging is strong for the

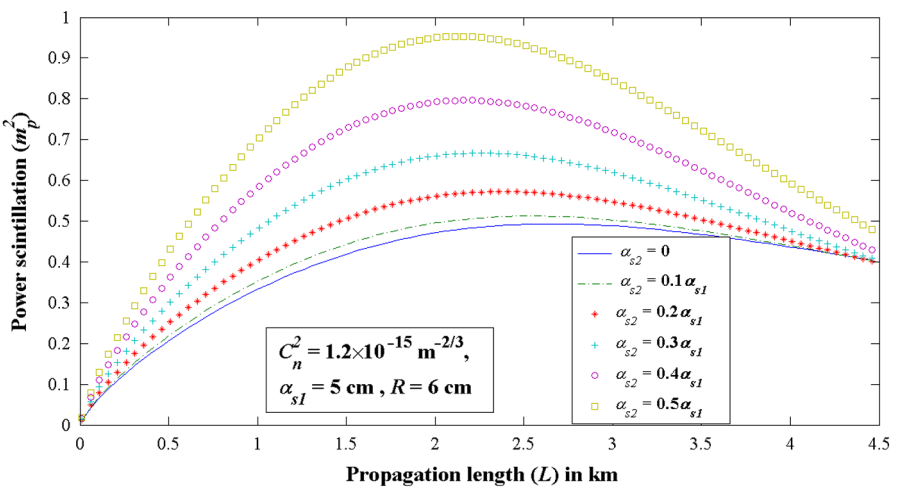

Fig. 3 Power scintillation versus the propagation length L at $C_n^2 = 1.2 \times 10^{-15}$ m$^{-2/3}$, $\alpha_{s1} = 5$ cm, and $R = 6$ cm for different α_{s2} values.

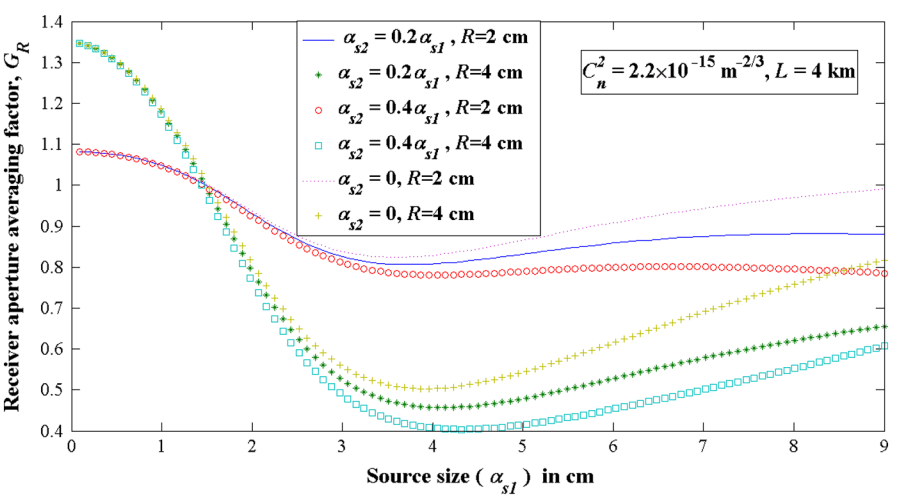

Fig. 4 The receiver-aperture averaging factor G_R versus the source size of the primary beam α_{s1} at $C_n^2 = 2.2 \times 10^{-15}$ m$^{-2/3}$ and $L = 4$ km for different source sizes of the secondary beam α_{s2} and different R values.

Downloaded From: http://opticalengineering.spiedigitallibrary.org/ on 03/02/2017 Terms of Use: http://spiedigitallibrary.org/ss/termsofuse.aspx

beams having larger apertures at the receiver plane and when the source size of the secondary beam increases, i.e., when the annular beam becomes thinner. It is also seen from Fig. 4 that the annular beams are more advantageous than the Gaussian beams ($\alpha_{s2} = 0$) when compared with respect to the effect of the receiver-aperture averaging. When Fig. 4 is compared with Fig. 3, although Gaussian beams have less power scintillation in Fig. 3, it is concluded from Fig. 4 that the decrease in the power scintillation is more for the annular beams, i.e., receiver-aperture averaging is more effective for the annular beam as compared with the Gausian beam.

Finally, we plot in Fig. 5 the receiver-aperture averaging factor versus the radius of the receiver aperture for annular and Gaussian beams at $L = 3$ km, where the source size of the primary beam is taken to be $\alpha_{s1} = 5$ cm and the source sizes of the secondary beam are taken different for the annular beams. It is concluded from Fig. 5 that with increasing values of the receiver-aperture sizes, the effect of the receiver-aperture averaging becomes stronger, as expected. When the annular beams and the Gaussian beam ($\alpha_{s2} = 0$) are compared, since increasing source sizes of the secondary beam promotes the effect of the receiver-aperture averaging, it is concluded that the annular beams are more favorable than the Gaussian beams.

We note that in order to observe effective receiver-aperture averaging factor, turbulence should not be very weak. Within the definition given in Eq. (11), the power scintillation index measured by a finite receiver-aperture, which depends on factors such as diffraction, propagation length, the shape of the incident beam, and turbulence strength, can yield larger values than the scintillation index measured by a point detector. Still staying in the weak turbulence regime but increasing the propagation length, when the structure is constant, and decreasing the wavelength, the receiver-aperture averaging factor always appears to be smaller than unity. To show this, we provide Fig. 5(b) which is plotted by employing our formulation in the current article to match Fig. 10.13 of Ref. 21, which is Fig. 6.10 of Ref. 18. In Ref. 21, the wavelength and the Gaussian source size values are taken as $\lambda = 0.633$ μm and $\alpha_s = 0.707$ cm. As the wavelength decreases, the Rytov intensity variance and the effect of the receiver-aperture averaging factor increase. If the wavelength decreases, the Rytov intensity variance and the effect of the receiver-aperture averaging increase. Figure 5(b) shows the receiver-aperture averaging factor versus the receiver-aperture radius scaled by the Fresnel zone for the Gaussian beam propagating in the turbulent atmosphere. The structure constant, the Gaussian source size, the propagation length, and the wavelength values are taken as $C_n^2 = 1.15 \times 10^{-14}$ m$^{-2/3}$, $\alpha_s = 0.707$ cm, $L = 1$ km, and $\lambda = 0.633$ μm, respectively. The receiver-aperture radius is taken from 0 to 10 cm. For these values, the Rytov intensity variance is calculated as $\sigma_R^2 = 0.65$. In Fig. 5(b), D is defined in Ref. 18 as the receiver-aperture radius, which corresponds to R in our current article. Figure 5(b), which is plotted by employing our formulation in the current article, is seen to perfectly match Fig. 10.13 of Ref. 21 (Fig. 6.10 of Ref. 18).

In some sections of Figs. 4 and 5(a), we observe that the receiver-aperture averaging factor is larger than unity. This means that the receiver-aperture averaging is not effective in those regions of the plots. The aperture averaging factor of a canonical beam such as a Gaussian beam being larger than unity at any parameter range, i.e., the scintillations detected by a finite size aperture receiver being larger than the scintillations detected by a point receiver, may not be plausible. We attribute this discrepancy in our findings to the inaccuracy in the structure and correlation functions involved in the employed fourth-order medium coherence function defined in Eq. (8). We note that by further investigating Eq. 10. 13 of Ref. 21, we have found that the receiver-aperture averaging factor is larger than unity in some cases.

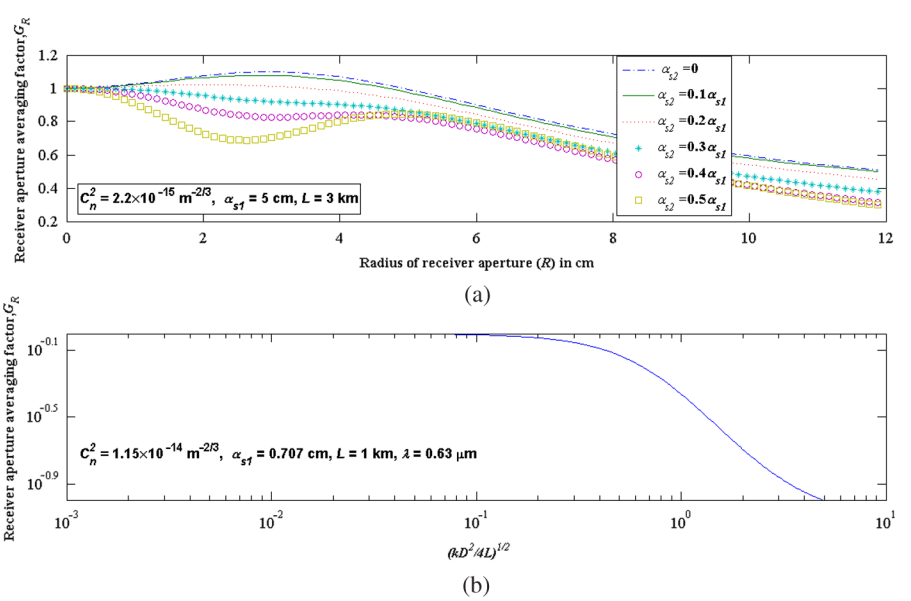

Fig. 5 (a) The receiver-aperture averaging factor G_R versus radius of the receiver aperture R at $C_n^2 = 2.2 \times 10^{-15}$ m$^{-2/3}$, $\alpha_{s1} = 5$ cm, and $L = 3$ km for different secondary beam source sizes. (b) Reproduction of Fig. 10.13 of Ref. 21, which is Fig. 6.10 of Ref. 18, by using our formulation in the current article.

Downloaded From: http://opticalengineering.spiedigitallibrary.org/ on 03/02/2017 Terms of Use: http://spiedigitallibrary.org/ss/termsofuse.aspx

For example, when Eq. 10. 13 of Ref. 21 is evaluated for $C_n^2 = 3 \times 10^{-15}$ m$^{-2/3}$, $\alpha_s = 3.8$ cm, $L = 3$ km, and $\lambda = 1.55$ μm, the receiver-aperture averaging factor is evaluated to be larger than unity for smaller receiver-aperture radii.

4 Conclusion

In this article, we calculated the power scintillation and the receiver-aperture averaging factor of annular beams propagating through a turbulent atmosphere. Consistent results are obtained when the aperture on the receiver plane is taken as a point detector, as in Refs. 10 and 11, or the propagating beam is a Gaussian beam having a finite aperture at the receiver plane,[2] as special cases. It is concluded from the results that annular beams are more advantageous than the Gaussian beams, since the effect of the receiver-aperture averaging is stronger for the annular incidences. Furthermore, increasing the secondary beam source size and the receiver-aperture radius promotes the effect of the receiver-aperture averaging. Increasing receiver-aperture radii also reduces and then smoothes the power scintillation index at large link lengths. The power scintillation index weakens from the middle of the link for large receiver-aperture radii.

References

1. V. I. Tatarskii, *The Effects of the Turbulent Atmosphere on Wave Propagation*, National Technical Information Service, Springfield (1971).
2. S. J. Wang, Y. Baykal, and M. A. Plonus, "Receiver-aperture averaging effects for the intensity fluctuation of a beam wave in the turbulent atmosphere," *J. Opt. Soc. Am.* **73**(6), 831–837 (1983).
3. J. C. Ricklin and F. M. Davidson, "Atmospheric optical communication with a Gaussian Schell beam," *J. Opt. Soc. Am. A* **20**(5), 856–865 (2003).
4. G. P. Berman, V. N. Gorshkov, and S. V. Torous, "Scintillation reduction for laser beams propagating through turbulent atmosphere," *J. Phys. B: At. Mol. Opt. Phys* **44**(5), 1–20 (2011).
5. R. Barrios and F. Dios, "Exponentiated Weibull distribution family under aperture averaging for Gaussian beam waves," *Opt. Express* **20**(12), 13055–13064 (2012).
6. X. Yi, Z. Liu, and P. Yue, "Average BER of free-space optical systems in turbulent atmosphere with exponentiated Weibull distribution," *Opt. Lett.* **37**(24), 5142–5144 (2012).
7. L. Dou, X. Ji, and P. Li, "Propagation of partially coherent annular beams with decentered field in turbulence along a slant path," *Opt. Express* **20**(8), 8417–8430 (2012).
8. C. Kamacıoğlu, Y. Baykal, and E. Yazgan, "Averaging of receiver aperture for flat-topped incidence," *Opt. Laser Technol.* **52**, 91–95 (2013).
9. Y. Baykal, "Log-amplitude and phase fluctuations of higher-order annular laser beams in a turbulent medium," *J. Opt. Soc. Am. A* **22**(4), 672–679 (2005).
10. H. T. Eyyuboğlu and Y. Baykal, "Scintillations of cos-Gaussian and annular beams," *J. Opt. Soc. Am. A* **24**(1), 156–162 (2007).
11. S. A. Arpali, H. T. Eyyuboğlu, and Y. Baykal, "Scintillation index of higher-order cos-Gaussian, cosh-Gaussian and annular beams," *J. Mod. Opt.* **55**(2), 227–239 (2008).
12. H. Gerçekcioğlu, Y. Baykal, and C. Nakiboğlu, "Annular beam scintillations in strong turbulence," *J. Opt. Soc. Am. A* **27**(8),1834–1839 (2010).
13. H. Gerçekcioğlu and Y. Baykal, "Annular beam scintillations in non-Kolmogorov weak turbulence," *Appl. Phys. B* **106**(4), 933–937 (2012).
14. M. A. Öztan, Y. Baykal, and C. Nakiboğlu, "Effects of extremely strong turbulent medium on scintillations of partially coherent annular and flat-topped Gaussian beams," *Opt. Commun.* **285**(6), 943–946 (2012).
15. Y. Baykal, H. T. Eyyuboğlu, and Y. Cai, "Scintillations of partially coherent multiple Gaussian beams in turbulence," *Appl. Opt.*, **48**(10), 1943–1954 (2009).
16. H. Gerçekcioğlu and Y. Baykal, "BER of annular and flat-topped beams in non-Kolmogorov weak turbulence," *Opt. Commun.* **286**, 30–33 (2013).
17. I. S. Gradshteyn and I. M. Ryzhik, *Tables of Integrals, Series and Products*, Academic Press Inc. (2000).
18. L. C. Andrews, R. L. Philips, and C. Y. Hopen, *Laser Beam Scintillation with Applications* SPIE Press (2001).
19. H. T. Eyyuboğlu, S. A. Arpali, and Y. Baykal, "Propagation characteristics of higher-order annular Gaussian beams in atmospheric turbulence," *Opt. Commun.* **264**(1), 25–34 (2006).
20. H. T. Eyyuboğlu, Y. Baykal, and E. Sermutlu, "Convergence of general beams into Gaussian intensity profiles after propagation in turbulent atmosphere," *Opt. Commun.* **265**, 399–405 (2006).
21. L. C. Andrews and R. L. Phillips, *Laser Beam Propagation through Random Media*, SPIE Press, Bellingham, Washington (2005).

Biographies and photographs of the authors are not available.

Downloaded From: http://opticalengineering.spiedigitallibrary.org/ on 03/02/2017 Terms of Use: http://spiedigitallibrary.org/ss/termsofuse.aspx